JOURNAL OF PROPULSION AND POWER
Vol. 21, No. 5, September–October 2005

# Systematic Design Approach for Radial Blade Regenerative Turbomachines

Muhammad M. Raheel* and Abraham Engeda†
*Michigan State University, East Lansing, Michigan 48823*

**The fundamentals, geometry, hypothesis of operation, applications, design procedure, current performance, and future trends of regenerative flow compressors (RFCs) and pumps are discussed. It has been suggested that regenerative turbomachines overcome various shortcomings of positive displacement and centrifugal turbomachines and are very good choices under certain operating conditions. Application of regenerative pumps in automotive fuel pumping and application of regenerative compressors in microturbines is discussed. A mathematical model to analyze the complex fluid motion inside regenerative turbomachines is presented. Various sources of losses are identified and quantified. Governing equations and loss models are utilized to develop a performance prediction code for regenerative turbomachines. Performance of a multistage RFC is predicted theoretically and compared with experimental data to validate the proposed model. The important geometric parameters affecting performance of regenerative turbomachines are listed. A design procedure for single- and multistage regenerative turbomachines with radial blades is proposed based on findings from theoretical analysis, experimental data available in literature, and analysis of existing regenerative turbomachine geometries. Several design criteria are established for the first time. The design procedure enables engineers working in regenerative turbomachinery to size various important dimensions of regenerative compressors and pumps. Finally, an overview of ongoing research and future direction is laid down.**

## Nomenclature

| | | |
|---|---|---|
| $A$ | = | area |
| $a$ | = | blade depth |
| $C$ | = | clearance |
| $D$ | = | diameter |
| $k$ | = | loss coefficient |
| $M$ | = | Mach number |
| $\dot{m}$ | = | through mass flow rate |
| $P$ | = | power |
| $p$ | = | pressure |
| $Q$ | = | through volume flow rate |
| $R$ | = | gas constant |
| $T$ | = | temperature |
| $t$ | = | blade thickness |
| $U$ | = | impeller velocity |
| $V$ | = | fluid velocity |
| $\alpha$ | = | shock loss parameter |
| $\Gamma$ | = | blade profile radius |
| $\gamma$ | = | ratio of specific heats |
| $\eta$ | = | isothermal efficiency |
| $\theta$ | = | peripheral angle |
| $\lambda$ | = | friction factor |
| $\nu$ | = | kinematic viscosity |
| $\rho$ | = | fluid density |
| $\sigma$ | = | slip factor |
| T | = | torque |
| $\Phi$ | = | specific mass flow rate |
| $\omega$ | = | rotational speed, rpm |

*Subscripts*

| | | |
|---|---|---|
| $a$ | = | axial direction |
| $b$ | = | blade |
| $c$ | = | circulatory direction |
| ch | = | channel |
| $f$ | = | curved surface |
| $g$ | = | centroidal |
| $h$ | = | hydraulic |
| in | = | compressor inlet |
| iso | = | isothermal |
| out | = | compressor outlet |
| $p$ | = | pumping |
| $r$ | = | radial direction |
| $s$ | = | stripper |

## Introduction

REGENERATIVE flow compressors and regenerative flow pumps (RFC/RFP) have found many applications in industry; still they are the most neglected in the family of dynamic turbomachines. Their main characteristic is ability to generate high heads at low flow rates. They have a very low specific speed and share some of the characteristics of positive displacement machines such as a roots blower, but without problems of lubrication and wear.

A typical cross section of a regenerative turbomachine is shown in Fig. 1 (Ref. 1). The flow resembles a corkscrew pattern as shown in (Fig. 1) with the help of a streamline passing though the impeller. In contrast to other popular types of continuous flow turbomachines in which fluid passes through the impeller once, regenerative turbomachines have fluid exposed to the impeller many times. The repetition of action of the impeller blading on the fluid is in effect multistaging, which makes them capable of developing high heads in a single stage. There is additional energy imparted to the fluid each time it passes through the blades of the impeller, allowing substantially more motive force to be added, which enables much higher pressures to be achieved in a more compact design. Each passage through the vanes may be regarded as a conventional stage of compression. This regenerative flow pattern of these turbomachines was first explained by Wilson et al.[2]

The essential elements of a typical regenerative turbomachine are shown in Fig. 2. An enlarged view of section A-A is shown in

Received 25 March 2003; revision received 10 January 2005; accepted for publication 3 March 2005. 

*Research Assistant, Turbomachinery Laboratory, Mechanical Engineering Department.
†Professor, Turbomachinery Laboratory, Mechanical Engineering Department.

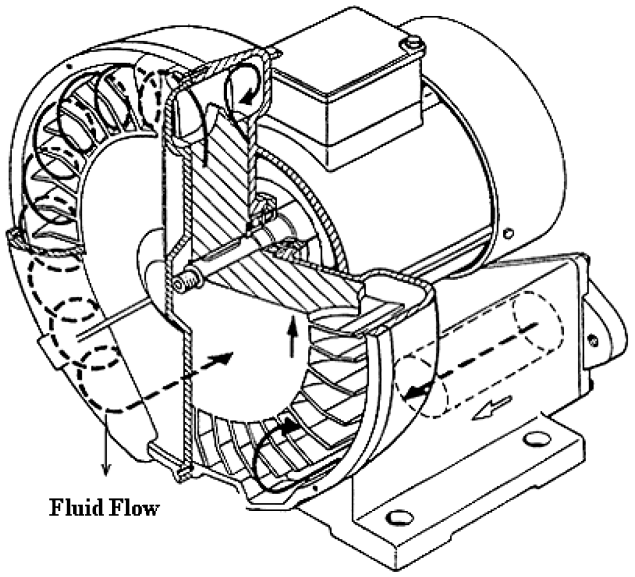


**Fig. 1 Regenerative turbomachine (Mugele[1]).**

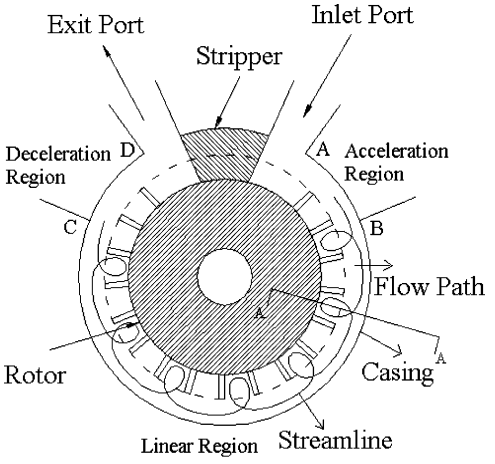


**Fig. 2 Elements of a regenerative turbomachine.**

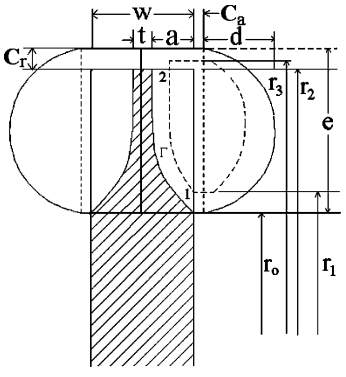


**Fig. 3 Section A-A enlarged.**

Fig. 3, which shows flow around a blade. Typically, a regenerative turbomachine has an impeller, inlet port, discharge port, stripper, flow passage, and casing. Regenerative turbomachines use a free rotating impeller just like other types of rotating turbomachines. The impeller has blades machined into each side at its periphery, which produce a series of helical flows, returning the fluid repeatedly through the blades for additional energy as it passes through an open annular channel. Inlet and discharge ports connect the external system piping to the flow channel. Fluid enters the flow channel via the inlet port, which is shaped to set up spiral flow around the annular channel. Fluid at high pressure is discharged to the piping

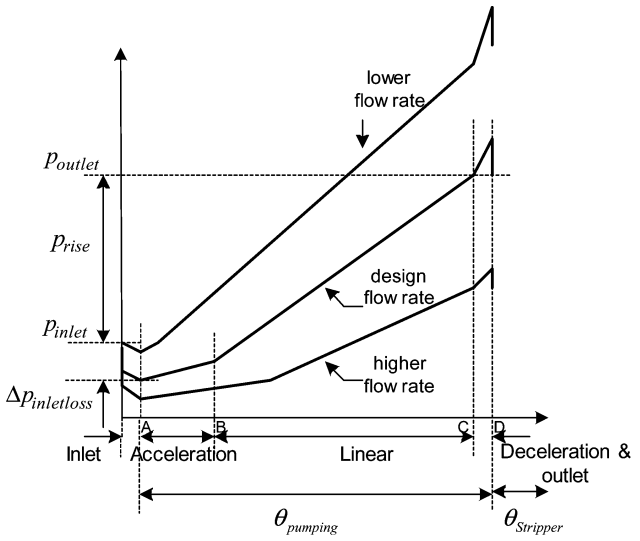


**Fig. 4 Tangential pressure variation in regenerative turbomachine.**

from the discharge port. Between the discharge and inlet, the casing clearance is reduced to block the high-pressure discharge from the low-pressure inlet. At this region, which is also known as the stripper, the open channel closes to within a few thousandths of an inch of the sides and tip of the rotor and allows only the fluid within the impeller to pass through the suction. Clearances between the impeller disk and casing are kept to a minimum to prevent leakage from the high-pressure side of RFC/RFP back to low-pressure side. The stripper forces the fluid to go out through discharge port. The stripper also helps in the establishment and maintenance of the regenerative flow pattern. Around the greater portion of the periphery, impeller blades project into an annular channel built in the casing. The flow channel has cross-sectional area greater than that of the impeller vanes. It is this annular flow channel from which fluid circulates repeatedly through the impeller blades. The fluid between the blades is thrown out and across the annular channel. Pressure variation of the fluid as it circulates through a regenerative turbomachine for several flow rates is shown in Fig. 4. These curves suggest five regions in the pump operation, which are also marked in Fig. 2.

1) In the inlet region (Fig. 4, A), the flow experiences some pressure loss.

2) In the acceleration region (Fig. 4, A–B), the flow enters the working section of turbomachine with a velocity and pressure dependent largely on the inlet region.

3) The pressure gradient is constant as indicated in the linear region, Fig. 4, B–C. This region is referred to as the working section of the pump, where the flow pattern is fully developed.

4) In the deceleration region (Fig. 4, C–D), a deceleration occurs, and the kinetic energy of the circulatory velocity is changed as a pressure rise. Therefore, there is a little pressure rise, as shown in Fig. 4.

5) In the outlet region (Fig. 4, D), a loss similar to that at the inlet region occurs.

Regenerative turbomachines are not known to have the best of efficiencies primarily because the circulatory flow pattern causes various types of losses. Typically regenerative compressors have an isothermal efficiency of less than 50%, but still they have found many applications because they allow the use of fluid dynamic compressors in place of positive displacement compressors for duties requiring high head and low flow rates. Most regenerative pumps reported in literature have less than 50% hydraulic efficiency. Although regenerative turbomachines are relatively less efficient, their simplicity of construction, stable operating characteristics, reliability, compact size, and low maintenance are making them more attractive to users in several areas. Recently they have found increasing use in microturbines, automotive and aerospace fuel pumping, booster systems, water supply, agricultural industries, shipping and mining, chemical and food stuffs industries, regulation of lubrication

and filtering, cryogenic applications in space vehicles, hydrogen gas pipelines, accessory drives on aircraft and missiles, and other applications as regenerative blowers. More applications of regenerative turbomachines may be found in Ref. 3. The two most common applications of regenerative turbomachines are discussed in the sequel.

## Application of RFP in Automotive Fuel Pumping

Fuel pumps for automotive applications have requirements for very high pressure rise at very low volumetric flow rates. To achieve this, regenerative fuel pumps are found to be more useful than any other available pumps. Regenerative pumps achieve very high pressure rise and typically operate at peak hydraulic efficiency of 40%. Because of their low specific speed, regenerative pumps allow high heads at low flow rates and present performance curves with very stable features. There are many reasons for the competitive advantage enjoyed by regenerative pumps over its competitor pumps.

1) The biggest advantage offered by a regenerative pump is its extremely compact design. Typical regenerative fuel pumps employed in automotives are less than 40 mm in diameter, which makes the pump motor assembly very compact. This feature is very attractive in automotives because of space limitations.

2) The self-priming capability offered by regenerative automotive fuel pump makes it very attractive. They have an ability to purge out vapors at start of pump operation and draw liquid fuel inside the impeller, something, which other fuel pumps lack. Regenerative pumps are known to have excellent priming behavior.

3) Operation at high fuel temperature is another huge advantage offered by these pumps. The fuel coming back from the injection system through the return line is very hot and, thus, requires the pump to operate at higher temperatures. Regenerative pumps are well known to handle high-temperature fuels.

4) Simplicity in construction is another huge advantage offered by these pumps.

5) They are very cheap to manufacture.

6) Ignition safety is another advantage offered by regenerative pumps.

7) Regenerative automotive fuel pumps are very durable. They have been tested to operate up to 10,000 h without any problems.

8) Low noise level is another highly desired attribute in automotives. RFP are very quiet and present a huge advantage over other fuel pumps.

9) There are no wearing problems in RFP like those found in positive displacement machines.

## Application to RFC in Microturbines

Microturbines are small combustion turbines, with outputs of 25–200 kW and can be located on sites with space limitations for power production. Microturbine application area has recently expanded to include distributed power generation, combined heat and power (cogeneration), offshore rigs, hospitals, backup generators, and hybrid vehicle applications. Microturbines are composed of a compressor, combustor, turbine, alternator, recuperator, generator, and fuel gas pressure booster compressor. If natural gas is used as fuel in the combustor, it provides the advantage of less cost, no storage problems, cleaner burning, less $NO_x$ emissions, and above all provision of higher efficiency and more power output than with any other gaseous fuel. A major problem with the use of natural gas is that it must be compressed enough to enter the combustor, and known gas compressors are very expensive and require significant energy to run. Most of the available compressors are screw-type or reciprocating compressors. These are generally equipped with gas coolers, oil separators, and accumulators. Because of high costs, it is desirable to provide a cheap method and apparatus for compressing the gas in a manner that eliminates typical problems associated with screw type or reciprocating compressors and also maintains the required concentration of natural gas in the mixture, which is injected into the combustor. Natural gas coming from pipelines in a residential or commercial area is kept at very low pressure, $\approx$0.2 psig, for fire safety reasons. Natural gas is required to be supplied to the combustor nozzle manifold at pressure as low as 1 psig (108 KPa). Typical gaseous fuel–air requirements are 20:1. Centrifugal compressors meet requirements of oil-free operation, no rubbing shafts and seals, and no sliding surfaces; however, centrifugal compressors operate best (with high efficiencies) when they have a high through flow rate and a low pressure rise relative to their tip speed. These operating conditions are characterized as high specific speed conditions. Highest efficiency is generally achieved at moderate specific speeds. Under these conditions, a centrifugal compressor can operate with efficiency on the order of 78%. However, for the operating conditions needed for microturbine operation, a centrifugal compressor can only provide an efficiency of 20%. Under these low flow and high head conditions, a centrifugal compressor would need as many as 10 stages to produce the same pressure rise for a given tip speed as a single-stage RFC can produce. Regenerative compressors provide simple, reliable design with only one rotating assembly. Operation is stable and surge free over a wide range. They have a long life, which is mainly dependent on bearing life. They require fewer stages when compared to centrifugal compressors. Moreover, they have higher efficiencies when compared to very low specific speed centrifugal compressors. RFC operating at low specific speed and at its best operating flow range can have efficiencies of about 55% with aerofoil blades and efficiencies of about 38% with straight radial blades. Requirements of the microturbine systems are low fuel flow and high discharge head. RFC overcomes all of the shortcomings of typical compressors that can be used for microturbine operation. This makes it a good match for the fuel compression requirements in a microturbine system.

Very few mathematical models in literature explain the behavior of regenerative turbomachines and predict the performance. Most of these models need extensive experimental support for performance prediction. Hence, it is interesting from an industrial standpoint to find efficient theoretical means that are able to forecast the regenerative turbomachine performances using easy to find geometric and fluid dynamic parameters.

Wilson et al.[2] presents a simplified model to permit the development of a theoretical analysis of the three-dimensional fluid motion inside a regenerative pump. The basic model developed in Ref. 2 was to represent the phenomenon in the linear region as shown in Fig. 4. They made several assumptions and applied fluid dynamic equations to arbitrary control volumes of the pump. The entire pump flow was characterized by tangential velocity $V_t$ and circulatory velocity $V_c$ along a mean streamline. Dimensionless performance characteristics for the STA-RITE TH 7 regenerative pump were tested and reported.[2] Experimental plots of flow vs head were obtained at seven different speeds with air as working fluid. Calculated and experimental performance curves were compared, and excellent agreement was observed. Qualitatively, the relations presented by Wilson et al. satisfied major details of the observed flow phenomena, but they needed extensive experimental support to predict performance. The Wilson et al. model assumed incompressible flow; thus, it is unable to predict performance of compressors producing high pressure ratio. Moreover, this model lacked correlation of losses with geometric and aerodynamic parameters. In this paper, the authors have extended the work of Wilson et al. to incorporate compressible flow to predict the performance characteristics of multistage RFC employed by Capstone Turbine Corporation for compression of natural gas for its Model C30 microturbine. Moreover, the authors have done some one-dimensional loss modeling to correlate various losses with geometric and aerodynamic parameters, thus eliminating need of experimental support.

## Mathematical Model

Mathematical formulation is based on an arbitrary element of depth $dX_g = r_g d\theta$ in the peripheral direction of the compressor as shown in Fig. 5. Equations of motion can be derived by considering these arbitrary small elements of one side blade and channel. For simplicity in the presentation of the analysis, wall friction and other irreversibilities are introduced as head losses.

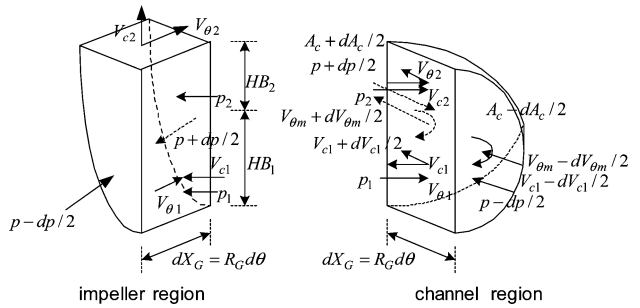


**Fig. 5 Control volumes representing section d$\theta$ of open channel and impeller.**

**Assumptions**

The following assumptions are made in the model.

1) The fluid is assumed incompressible within a control volume; however, from one control volume to the next, fluid density changes.

2) Fluid shear is assumed negligible in the model; however, it is considered in the calculation by assuming a model for tangential head loss.

3) Steady flow without any leakage is assumed. Leakages are considered separately to avoid complexity in the basic model.

4) Characteristic flow is one dimensional in which the major direction is radial, tangential, and axial.

5) There are no end effects of suction, discharge, and stripper carryover.

6) Tangential pressure gradient is independent of radius. Literature and experimental studies by Wilson et al.[2] have confirmed that this assumption is quite valid.

7) Although, the tangential pressure gradient around the periphery is not perfectly linear, for simplicity, assumption of linear pressure rise across the periphery is reasonable.

**Governing Equations**

The tangential components of velocity at points 1 and 2 where fluid streamline enters and discharges impeller blade can be given as

$$V_{\theta 1} = \alpha U_1 \tag{1}$$

$$V_{\theta 2} = \sigma U_2 \tag{2}$$

where $\alpha$ is a shock loss parameter introduced at blade entrance to quantify shock losses. More details on calculation of slip factor and shock loss parameter may be found by Raheel.[3]

Circulatory velocity at point 1 and 2 is assumed to be equal. Thus,

$$V_{c1} = V_{c2} = V_c \tag{3}$$

Circulatory flow rate can be approximated by

$$\mathrm{d}Q_c = C_r V_c \,\mathrm{d}X_g \tag{4}$$

Applying angular momentum equation to the impeller control volume of Fig. 5, we get

$$\mathrm{dT} = \rho \,\mathrm{d}Q_c (r_2 \sigma U_2 - r_1 \alpha U_1) + r_g A_b \frac{\mathrm{d}p}{\mathrm{d}\theta}\,\mathrm{d}\theta \tag{5}$$

The last term on the right hand side in Eq. (5) represents the work done in raising the pressure of the fluid between the impeller blades. This pressure rise is utilized across the stripper to perform the turbine work. Therefore, this term is ignored generally. Power input to the differential control volume can be given as

$$\mathrm{d}P = \omega \,\mathrm{dT} \tag{6}$$

Thus, we can write

$$\mathrm{d}P = \rho \,\mathrm{d}Q_c \left(\sigma U_2^2 - \alpha U_1^2\right) \tag{7}$$

Applying Bernoulli's equation to the impeller control volume in Fig. 5, we get

$$\mathrm{d}P = \rho \,\mathrm{d}Q_c \left[\left(\sigma^2 U_2^2/2\right) + \left(V_{c2}^2/2\right) + (p_2/\rho) - \left(\alpha^2 U_1^2/2\right) - \left(V_{c1}^2/2\right) - (p_1/\rho)\right] \tag{8}$$

Equations (7) and (8) yield

$$(p_1/\rho) + \left(V_{c1}^2/2\right) + \left(\alpha^2 U_1^2/2\right) + \sigma U_2^2 = (p_2/\rho) + \left(V_{c2}^2/2\right) + \left(\sigma^2 U_2^2/2\right) + \alpha U_1^2 + g H_{cb} \tag{9}$$

where $gH_{cb}$ is the head loss of circulatory velocity through the impeller region.

When the continuity equation is applied to the channel control volume shown in Fig. 5,

$$\rho(V_{\theta m} + \mathrm{d}V_{\theta m}/2)(A_c + \mathrm{d}A_c/2) + \rho \mathrm{d}Q_{c1} = \rho(V_{\theta m} - \mathrm{d}V_{\theta m}/2)(A_c - \mathrm{d}A_c/2) + \rho \mathrm{d}Q_{c2} \tag{10}$$

or

$$\mathrm{d}(V_{\theta m} A_c) = 0 \tag{11}$$

where $V_{\theta m}$ is mean tangential velocity, which can be obtained as

$$V_{\theta m} = Q/A_c \tag{12}$$

Angular momentum equation in the tangential direction yields

$$\rho r_g (V_{\theta m} + \mathrm{d}V_{\theta m}/2)(A_c + \mathrm{d}A_c/2)\,\mathrm{d}V_{\theta m} + \rho\,\mathrm{d}Q_c (r_1 V_{\theta 1} - r_2 V_{\theta 2}) = r_g (p - \mathrm{d}p/2)(A_c - \mathrm{d}A_c/2) - r_g (p + \mathrm{d}p/2)(A_c + \mathrm{d}A_c/2) + r_g p\,\mathrm{d}A_c - \text{wall friction term} \tag{13}$$

By use of continuity equation, Eq. (13) can be reduced to

$$\mathrm{d}gH = \mathrm{d}Q_c/Q_s (U_2 V_{\theta 2} - U_1 V_{\theta 1}) + V_{\theta m}^2\,\mathrm{d}A_c/A_c - \mathrm{d}gH_L \tag{14}$$

where $Q_s = \omega r_g A_c$ is flow rate based on solid body rotation.

In the right side of Eq. (14), the first term refers to head rise caused by momentum exchange of blade, the second term gives head rise caused by the deceleration of the mean tangential velocity, and the last term gives head loss caused by the friction and the contraction or expansion of the tangential velocity.

When the momentum equation is applied in the circulatory direction

$$\rho\,\mathrm{d}Q_{c1} V_{c1} - \rho\,\mathrm{d}Q_{c2} V_{c2} + \rho Q\,\mathrm{d}V_c = p_2 H B_2\,\mathrm{d}X_2 - p_1 H B_1\,\mathrm{d}X_1 - \text{wall friction term} \tag{15}$$

$$\frac{Q V_c\,\mathrm{d}V_c}{\mathrm{d}Q_c} = \frac{p_2 - p_1}{\rho} - g H_{cc} \tag{16}$$

where $gH_{cc}$ is the head loss of circulatory velocity through the impeller region.

The energy equation applied to channel control volume shown in Fig. 5 after some simplifications yields

$$\frac{p_2}{\rho} + \frac{V_{c2}^2}{2} + \frac{\sigma^2 U_2^2}{2} = \frac{p_1}{\rho} + \frac{V_{c1}^2}{2} + \frac{\alpha^2 U_1^2}{2} + g H_{cc} + \frac{Q}{\mathrm{d}Q_c}\left(\mathrm{d}gH + \mathrm{d}gH_L - \frac{V_{\theta m}^2\,\mathrm{d}A_c}{A_c} + V_c\,\mathrm{d}V_c\right) \tag{17}$$

If Eqs. (9), (14), and (16) are used in Eq. (17), the first-order nonlinear ordinary differential equation for the circulatory flow can be obtained as follows:

$$\frac{Q V_c\,\mathrm{d}V_c}{\mathrm{d}Q_c} = \left(1 - \frac{Q}{Q_s}\right)\left(\sigma V_{\theta 2}^2 - \alpha V_{\theta 1}^2\right) - g H_c \tag{18}$$

where $gH_c = gH_{cb} + gH_{cc}$ is the sum of head loss related to the circulatory velocity.

**Shock and Slip Losses**

The tangential pressure gradient in regenerative turbomachines enhances the slip factor considerably. The pressure difference between any two adjacent blades of an impeller causes a tendency for a secondary circulation about each blade such that the fluid leaving the impeller deviates from the path prescribed by the blade surface, backward with respect to the positive direction of impeller rotation. The result is that the fluid tangential velocity at exit is less than that which would be expected from the velocity triangle based on the outlet blade angle. To allow for the reduction in the ideal tangential velocity, a slip factor is usually introduced. It is defined as the ratio between actual tangential velocity and the one obtained with the assumption that the flow angle and blade angle are identical. In present investigation, a model for the calculation of slip factor for regenerative turbomachines is introduced, details of which can be found by Raheel.[3] Shock or incidence losses are caused by difference between blade angle and flow angle when fluid enters the blades. Wilson et al.[2] introduced a shock loss parameter $\alpha$ to quantify such losses. The Wilson et al. model is used in this work to calculate shock losses.

**Circulatory Head Losses**

Circulatory head losses have two contributions: 1) Head loss of circulatory velocity through the impeller region is referred as $gH_{cb}$. 2) Head loss of circulatory velocity through the channel region is referred as $gH_{cc}$. The sum of these two head losses is the total circulatory head loss given as

$$gH_c = gH_{cb} + gH_{cc} \tag{19}$$

Circulatory head losses arise from many sources. The following sources of circulatory head loss were quantified. Details may be found in Ref. 3.

Channel turning losses $k_t$ are due to the 180-deg turn of the fluid through the channel.

Blade turning losses $k_b$ are due to the turning of fluid through the impeller blades.

Channel and blade mixing losses $k_{ch}$ and $k_s$ occur due to the mixing of fluid leaving the tip of the impeller blade and mixing with the incoming stream of flow through the channel.

Sudden expansion losses $k_{\text{se}}$ are caused by the sudden increase in flow area when fluid flows from blades to channel.

Consequently, model for the circulatory head loss can be arranged as follows:

$$gH_c = \tfrac{1}{2}k_t V_c^2 + \tfrac{1}{2}k_b V_c^2 + \tfrac{1}{2}k_{ch} V_c^2 + \tfrac{1}{2}k_s V_{\theta m}^2 + \tfrac{1}{2}k_{\text{se}} V_c^2 \tag{20}$$

The various loss coefficients in Eq. (20) are correlated with geometric and aerodynamic parameters in Ref. 3.

**Tangential Head Losses**

Head losses caused by channel friction are referred as tangential head losses denoted by $\mathrm{d}gH_L$. They involve the channel curvature effect and can be determined by applying the classic pipe-loss formula:

$$\mathrm{d}gH_L = \frac{\lambda_f V_{\theta m}^2 \, \mathrm{d}X_g}{2D_h} \tag{21}$$

where $\lambda_f$ is the friction factor for the curved surface given as

$$\lambda_f = \lambda_0 \left(1 + 0.075 Re^{0.25} (D_h/2r_2)^{0.5}\right) \tag{22}$$

and $\lambda_0$ is defined for the straight channel as

$$\lambda_0 = 0.316 Re^{-0.25} \tag{23}$$

where Reynolds number is given based on hydraulic diameter as

$$Re = D_h V_{\theta m}/\nu \tag{24}$$

**Leakage Losses**

Total leakage flow rate can be estimated by the following equation suggested by El-Hag[4]:

$$Q_{\text{leak}} = \frac{\omega r_2}{2} - \left(C_r a + \frac{C_a r_2}{2}\right) + 2C_D \omega r_2 \sqrt{2\frac{\mathrm{d}\Psi}{\mathrm{d}\theta} \Big/ Z_s}$$
$$\times [C_r(b + C_a) + C_a(r_2 - r_0)] \tag{25}$$

where $C_D$ is orifice discharge coefficient.

**Losses in Ports**

Losses in inlet and discharge ports are estimated as follows.

Inlet port:

$$\Delta P_{\text{in}} = \tfrac{1}{2} K_{\text{in}} \rho V_{\text{in}}^2 \tag{26}$$

Outlet port:

$$\Delta P_{\text{out}} = \tfrac{1}{2} K_{\text{out}} \rho V_{\text{out}}^2 \tag{27}$$

The two loss coefficients $K_{\text{in}}$ and $K_{\text{out}}$ need to be correlated with the nozzle geometries and flow rates to study the effect of inlet and discharge ports on performance. The effect of inlet and discharge manifold is not the primary aim of this work, and so the authors did not correlate these loss coefficients with aerodynamic parameters. Instead, reasonable values of these coefficients were assumed and held constant during computations.

## Performance Prediction and Comparison with Test Data

Based on proposed mathematical model and loss correlations, a performance prediction code for regenerative turbomachines is developed. Mathematical formulation is based on some geometrical parameters, which are the input to the code. More detail on the code organization and solution procedure can be found by Raheel.[3] The performance prediction code predicts the pressure ratio for the entire operating range. To validate the proposed mathematical model, the geometry of a multistage RFC is used as input of the code, and theoretical results are compared to the experimental data. Excellent agreement between theoretical and experimental data is observed as shown in Figs. 6 and 7. Figures 6 and 7 represent theoretical and test data overlapped for natural gas as working fluid at four inlet pressures of 0 (101.325 KPa), 5 (135.8 KPa), 10 (170.3 KPa), and 15 (204.77 KPa) psig at inlet temperature of 70°F. To condense the presentation, only results at 195 and 250 standard *l*/min are provided. A sensitivity analysis is performed by varying various geometrical parameters to improve the performance of the multistage RFC. Details of this sensitivity analysis and suggestions for improvement in design may be found in Ref. 3.

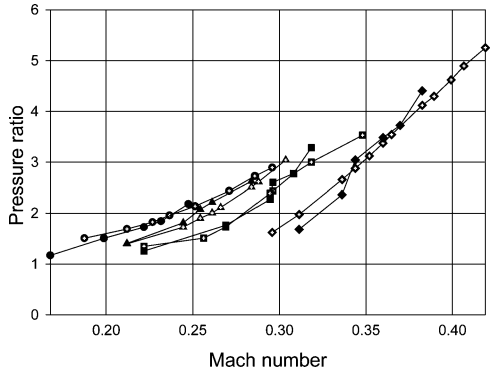


**Fig. 6 Theoretical and test data overlapped for flow rate 195 standard *l*/min: code prediction for $P_{\text{in}}$ = 15 psig (204.77 KPa), experimental result for $P_{\text{in}}$ = 15 psig (204.77 KPa); code prediction for $P_{\text{in}}$ = 10 psig (170.3 KPa), experimental result for $P_{\text{in}}$ = 10 psig (170.3 KPa); code prediction for $P_{\text{in}}$ = 5 psig (135.8 KPa), experimental result for $P_{\text{in}}$ = 5 psig (135.8 KPa); and code prediction for $P_{\text{in}}$ = 0 psig (101.325 KPa), experimental result for $P_{\text{in}}$ = 0 psig (101.325 KPa).**

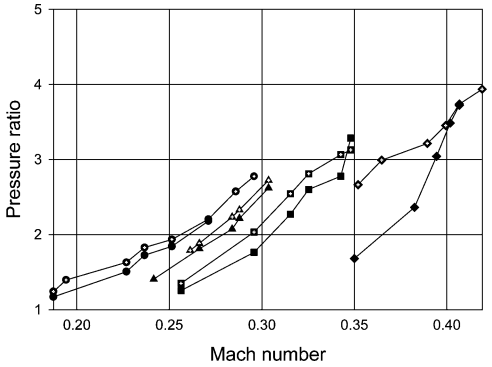


**Fig. 7 Theoretical and test data overlapped for flow rate 250 standard *l*/min: code prediction for $P_{in} = 15$ psig (204.77 KPa), experimental result for $P_{in} = 15$ psig (204.77 KPa); code prediction for $P_{in} = 10$ psig (170.3 KPa), experimental result for $P_{in} = 10$ psig (170.3 KPa); code prediction for $P_{in} = 5$ psig (135.8 KPa), experimental result for $P_{in} = 5$ psig (135.8 KPa); and code prediction for $P_{in} = 0$ psig (101.325 KPa), experimental result for $P_{in} = 0$ psig (101.325 KPa).**

## Design Approach

To make this discussion useful for designers and engineers working in the field of regenerative turbomachinery, a design approach is discussed in this paper for the first time. It is a standard practice in the turbomachinery field to select an operating point where the designer intends to achieve peak efficiency. Thus, as a starting point, a design point needs to be selected. Some nondimensional parameters are defined as follows.

Impeller tip Mach number:

$$M_{OT} = r_2\omega \Big/ \sqrt{\gamma R T_{\text{in}}} \tag{28}$$

Pressure ratio:

$$\Pi = P_{\text{out}}/P_{\text{in}} \tag{29}$$

Specific mass flow rate:

$$\Phi = \dot{m} \Big/ 4r_2^2 P_{\text{in}} \sqrt{RT_{\text{in}}/\gamma} \tag{30}$$

Isothermal efficiency:

$$\eta_{\text{iso}} = \frac{\dot{m} R T_{\text{in}}\, \ell n(P_{\text{out}}/P_{\text{in}})}{\text{power draw}} \tag{31}$$

To provide a guideline for designers to make a decent choice of operating point, the authors developed a correlation between pressure ratio, specific mass flow rate, and impeller tip Mach number from available experimental data on single-stage regenerative compressors with radial blades. This correlation is given as

$$\begin{aligned} &\Pi = 0.935 + 3.08 M_{OT}^{1.5} - (5.45 \times 10^5)\Phi^2 \\ &\text{regression coefficient } (r^2) = 0.991 \end{aligned} \tag{32}$$

The trend between these nondimensional parameters is shown in Fig. 8, which shows performance characteristics of a typical regenerative turbomachine. Let us assume that a single-stage regenerative compressor needs to be designed to meet following operating conditions: working fluid, air; $T_{\text{in}} = 294$ K; $P_{\text{in}} = 101{,}325$ N/m$^2$; $\dot{m} = 0.0035$ kg/s; and desired pressure ratio $\Pi = 1.4$. To use correlation (32), a reasonable assumption for impeller tip Mach number has to be made. It is reported by Cates[5] that compressibility effects that are detrimental to compressor efficiency start to come into play at $M_{OT} > 0.7$. From Fig. 8, note that to get a decent pressure ratio across the stage, the Mach number has to be greater than 0.3. It was concluded from the experimental data for single- and multistage compressors presented by Raheel et al.[6] and Cates[5] that as the Mach number increases beyond a certain limit, the efficiency starts to go down. Although pressure ratio increases with increasing Mach number, the circulatory and tangential head losses severely

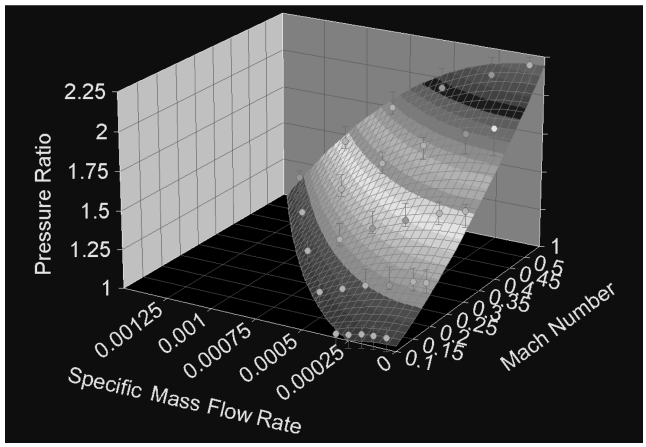


**Fig. 8 Pressure ratio vs specific mass flow rate and Mach number.**

affect efficiency at Mach number in excess of 0.5. Thus, for best performance, it is recommended to use

$$0.35 < M_{OT} < 0.45 \tag{33}$$

Assuming $M_{OT} = 0.4$ and using Eq. (32), we obtain $\Phi = 7.6 \times 10^{-4}$. Using Eqs. (28) and (30), we can obtain the impeller tip radius and compressor revolutions per minute (RPM) as

$$r_2 = 0.0528 \text{ m}$$

$$\text{RPM} = 24{,}866$$

If a designer feels that the size of compressor becomes undesirably large, the Mach number can be reduced. However, a reduction of Mach number will reduce the pressure ratio. After the determination of the impeller tip radius and operating speed, various impeller and channel dimensions have to be determined. Typically the channel area ratio is kept constant across the periphery for RFP design; however, due to density changes in RFC, the channel area decreases from inlet to discharge port. For this purpose, we define a station A at the start of linear region and a station B at the end of the linear region, as shown in Fig. 2. The channel depth and, hence, the channel area at station B is lower than station A. The important dimensions in the design of a regenerative turbomachine are radial clearance $C_r$; channel depth at station A, $d_A$; channel depth at station B, $d_B$; channel height $e$; area ratio, $A_{c,A}/A_{c,B}$; impeller radius ratio, $r_2/r_0$; blade depth $a$; blade profile radius $\Gamma$; blade thickness $t$; axial clearance $C_a$; and number of impeller blades, $Z$.

The authors have looked into test data published in literature, the test data on Capstone single and multistage RFC presented in Ref. 6, and theoretical results from performance prediction code to establish some design criteria for the mentioned parameters. Some authors in the past have done experimental sensitivity analysis on RFC/RFP dimensions. Their analysis is also considered while establishing design criteria.

#### Radial Clearance $C_r$

Radial clearance $C_r$ has an effect on three types of losses: shock loss, blade turning loss, and channel and blade mixing losses. The performance prediction code has been used to study the effect of radial clearance on various losses. Details of this sensitivity analysis may be found in Ref. 3. Figure 9 shows the variation of various loss coefficients with the ratio $C/r_2$. Note that tip radius was held constant while performing the sensitivity analysis for radial clearance. Shock loss is minimized by increasing radial clearance $C_r$. The shock loss parameter inversely affects the pressure ratio. To get higher pressure ratio and isothermal efficiency, the shock loss parameter should be as small as possible, and actually a negative value is beneficial because it increases the pressure ratio. Usually, at very low flow rates, negative values of $\alpha$ are obtained, which mean high pressure ratios are achieved.

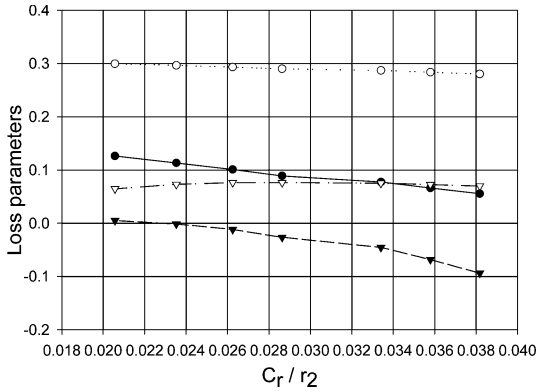


**Fig. 9 Various loss parameters vs $C_r/r_2$: ○, blade turning loss coefficient $k_b$ vs ratio $C_r/r_2$; ●, shock loss parameter $\alpha$ vs ratio $C_r/r_2$; ▽, blade mixing loss coefficient $k_m$ vs ratio $C_r/r_2$; and ▼, channel mixing loss coefficient $k_{ch}$ vs ratio $C_r/r_2$.**

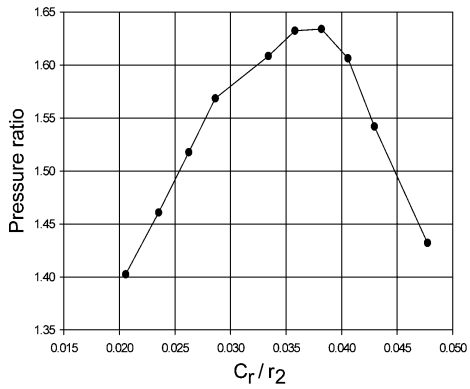


**Fig. 10 Pressure ratio vs $C_r/r_2$.**

Increasing radial clearance $C_r$ also minimizes blade turning loss. Channel and blade mixing losses are also affected with the change in radial clearance. The blade mixing loss does not show any obvious trend, and it is very hard to conclude that either increasing or decreasing radial clearance helps to reduce this loss. However, a definite trend is obvious in the channel mixing loss. Channel mixing loss becomes more negative with increasing radial clearance, which helps to increase pressure ratio and efficiency. To study the cumulative effect of the losses and the effect of radial clearance on pressure ratio, the pressure ratio for the first stage of the Capstone multistage RFC at the design point is plotted against ratio $C_r/r_2$ as shown in Fig. 10. Note that the pressure ratio increases with an increase in radial clearance $C_r$; however, after a certain percentage of increase, the pressure ratio actually starts going down. The findings from the sensitivity analysis were compared to experimental analysis presented by Cates[5] and Wilson et al.[2] and a design criterion has been established for sizing the radial clearance, given as

$$0.03 < C_r/r_2 < 0.05 \tag{34}$$

**Channel Depth at Station A, $d_A$**

Channel depth effects following losses: shock loss, channel turning loss, and skin-friction loss. Each of these losses was analyzed for variation in channel depth using the performance prediction code. More detail can be found in Ref. 3. After a sensitivity analysis was done from the code and based on test data presented by Cates,[5] Wilson et al.,[2] and Burton,[7] it was observed that large channel depth causes a sharp drop in efficiency. At low specific flow rate, it is beneficial to use small channel depth. A design criterion for selection of channel depth is

$$0.2 < C_r/d_A < 0.65 \tag{35}$$

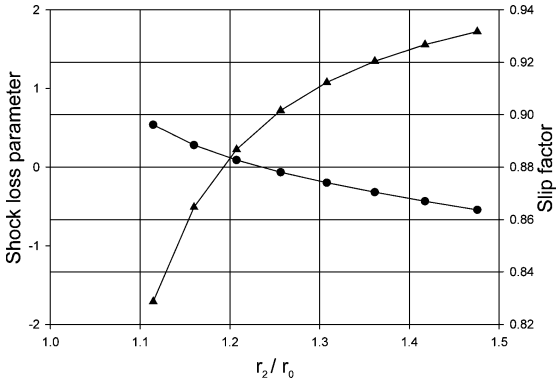


**Fig. 11 Slip and shock loss parameter vs impeller radius ratio: ●, shock loss parameter $\alpha$ vs impeller radius ratio and ▲, slip factor $\sigma$ vs impeller radius ratio.**

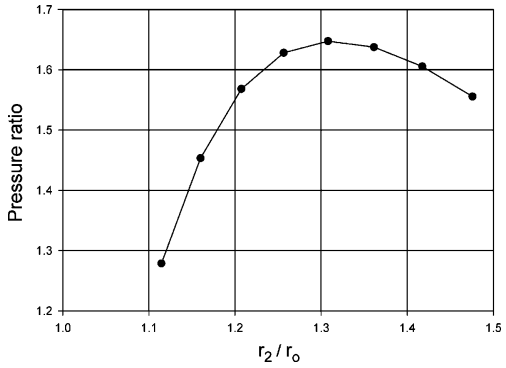


**Fig. 12 Pressure ratio vs impeller radius ratio.**

**Impeller Radius Ratio $r_2/r_0$**

Impeller tip radius is a very important geometric parameter for performance. It controls the overall size of the machine and also the impeller tip Mach number. Impeller tip radius affects two of the most important sources of losses, that is, slip and shock. It was found from the code that shock and slip losses are minimized by increasing the tip radius. Moreover, it was found that slip and shock losses can be reduced by making the impeller hub radius smaller. To see the cumulative effect, the authors performed an analysis on impeller radius ratio $r_2/r_0$. Slip factor, shock loss parameter, and pressure ratio are plotted against impeller radius ratio in Figs. 11 and 12. It is quite obvious that increasing the radius ratio is helpful for better performance. However, after a certain radius ratio, the pressure ratio starts to go down, as shown in Fig. 12. The impeller hub radius can be calculated using

$$r_0 = r_2 + C_r - 2d_A \tag{36}$$

However, the resulting value of $r_0$ should satisfy the following criterion:

$$1.1 < r_2/r_0 < 1.5 \tag{37}$$

**Channel Height $e$**

The channel height $e$ is a function of radial clearance and impeller tip radius. A simple way to determine channel height is using

$$e = r_2 - r_0 + C_r \tag{38}$$

**Area Ratio $A_{c,A}/A_{c,B}$**

Channel area at station A is a function of channel depth $d_A$. From the sensitivity analysis of the code, it is concluded that the higher the area ratio, the higher is the pressure ratio and efficiency at a given impeller tip Mach number. This has been validated by experimental test data presented in Ref. 5. It has been found through test data that a higher area ratio is beneficial for improved pressure ratio and isothermal efficiency. Figure 13 shows the increase in pressure ratio

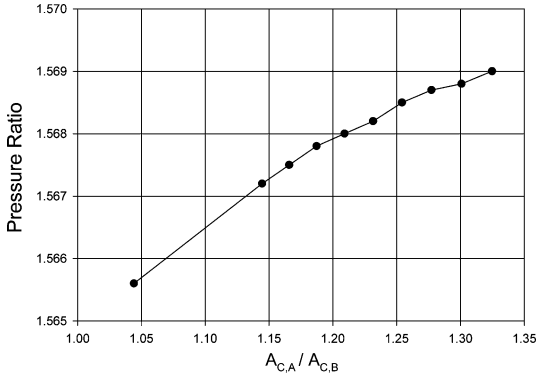


**Fig. 13 Pressure ratio vs channel area ratio.**

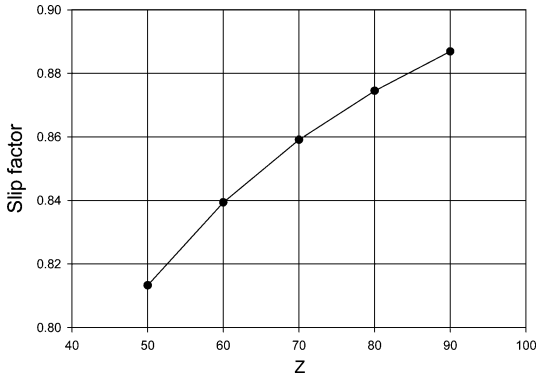


**Fig. 14 Slip factor vs number of blades.**

obtained by increasing the area ratio. The channel area at station A can be found by

$$A_{c,A} = \pi d_A^2 / 2 \tag{39}$$

A design criterion for channel area ratio has been established as

$$1.15 < A_{c,A}/A_{c,B} < 1.35 \tag{40}$$

The channel depth at station B can be found by

$$d_B = \sqrt{2A_{c,B}/\pi} \tag{41}$$

**Number of Impeller Blades, *Z***

Many researchers the most noteworthy of whom are Iverson[8] and Mason,[9] have investigated number of impeller blades. Blade number has an obvious effect on slip factor, as shown in Fig. 14. Slip losses are increased immensely when blade number is reduced, which has a very detrimental effect to pressure ratio and efficiency. A blade number between 75 and 90 seems reasonable for RFC/RFP design. Further increase in blade number might prove harmful because it will make the angle between blades less than 4 deg, which might not allow enough circulation through the impeller. Instead impeller will appear as a rough surface to the fluid, and there will be fewer circulations, making it difficult to produce the desired pressure ratio. Moreover, frictional losses can increase due to too many blades in the impeller. Figure 15 shows the improvement in pressure ratio with increasing blade number. It is suggested that the number of impeller blades must be selected using the following design criterion:

$$75 < Z < 90 \tag{42}$$

The preceding analysis has been performed for purely radial blade regenerative turbomachines. It has been suggested by many authors in the literature that, for best performance, the impeller blades should be chevroned at a certain angle. The blade chevron angle must be selected using the following design criterion:

$$45^\circ < \beta < 60^\circ \tag{43}$$

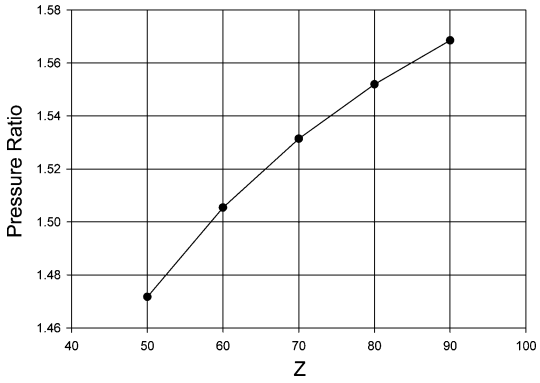


**Fig. 15 Pressure ratio vs number of blades.**

The blade depth, blade profile radius, blade thickness, and axial clearance can be designed using following criteria:

$$0.03 < a/r_2 < 0.13 \tag{44}$$

$$0.1 < \Gamma/r_2 < 0.2 \tag{45}$$

$$0.25 < t/a < 0.4 \tag{46}$$

$$0.0015 < C_a/r_2 < 0.003 \tag{47}$$

Based on the preceding discussion, a single-stage RFC has been designed at the selected design point. The calculations are provided in the Appendix. Individual stages of a multistage RFC can be designed in a similar manner. Raheel et al.[6] reported a correlation between impeller tip Mach number $M_{OT}$, specific mass flow rate $\Phi$, and pressure ratio $\Pi$ produced by a four-stage RFC as

$$\Pi = -5.6 + 47.13M_{OT} - 135.6M_{OT}^2 + 161.27M_{OT}^3 + 0.0019/\Phi \tag{48}$$

A correlation between impeller tip Mach number $M_{OT}$, specific mass flow rate $\Phi$, and isothermal efficiency $\eta$ produced by a multistage RFC is given as

$$\eta = 2.49 + (26.1/M_{OT}) - (0.064/\Phi) - \left(3.77/M_{OT}^2\right) - (1.51 \times 10^{-6}/\Phi^2) + [0.0121/(\Phi)(M_{OT})] \tag{49}$$

These correlations provide a starting point in the design of a multistage RFC. The conditions at the exit of the first stage can be approximated as inlet conditions for the second stage for design purposes.

In turbomachinery design, one-dimensional codes are typically used to size various dimensions, which are later optimized by computational fluid dynamics (CFD) analysis. The presented design criteria can serve as a good starting point in RFC/RFP design; however, a CFD analysis must be performed to make necessary design improvements before a prototype can be built.

## Conclusions

An introduction to the fundamentals of regenerative turbomachines is presented. It has been suggested that RFC/RFP are very good choices under certain operating conditions,[1] where reciprocating and centrifugal turbomachines are not as well suited. There is a great potential in regenerative turbomachines for various industries. A mathematical model to describe the fluid motion inside regenerative turbomachines is discussed. The mathematical model has been validated by comparing theoretical results with experimental data on a multistage RFC. A design procedure for RFC/RFP is outlined. Various correlations and design criteria are introduced, which facilitate the design process. Based on the design criteria, a sample calculation for single-stage compressor design at a selected design point is presented. The resulting design is a starting point for CFD analysis, which must be performed to optimize the design before actual prototype can be built and tested.

The biggest challenge faced with regenerative turbomachines is to improve their efficiencies to the level enjoyed by centrifugal compressors and pumps to make them more competitive. The future direction in regenerative turbomachinery design is to improve these design criteria. More design guidelines must be developed to facilitate the RFC/RFP design procedure. The flow guidance inside regenerative turbomachines must be improved using commercial CFD codes. The geometries resulting from one-dimensional analysis must be improved using CFD analysis for best performance. The authors have conducted CFD analysis on a regenerative automotive fuel pump and an aerofoil blade RFC design. Details of this analysis will be presented in another publication to appear soon.

## Appendix: Example Design Calculation

Where $r_2 = 2.0$ in. and for 24,850 rpm, assume $C_r/r_2 = 0.038$. Using Eq. (34), we get $C_r = 0.076$ in. Assume $C_r/d_A = 0.447$, and using Eq. (35), we get $d_A = 0.17$ in. Using Eq. (36), we get $r_0 = 1.736$ in. When Eq. (37) is checked, $r_2/r_0 = 1.15$. Thus, it satisfies the criteria for radius ratio. Using Eq. (38), we get $e = 0.34$ in. Using Eq. (39), we get $A_{c,A} = 0.0453$ in.$^2$ Assume $A_{c,A}/A_{c,B} = 1.25$, and using Eq. (40), we get $A_{c,B} = 0.036$ in.$^2$ Using Eq. (41), we get $d_B = 0.151$ in. Using Eq. (42), select $Z = 81$. Using Eq. (43), select $\beta = 55$. Assume $a/r_2 = 0.07$, and using Eq. (44), we get $a = 0.145$ in. Assume $\Gamma/r_2 = 0.19$, and using Eq. (45), we get $\Gamma = 0.38$ in. Assume $t/a = 0.3$, and using Eq. (46), we get $\Rightarrow$ $t = 0.0435$ in. Assume $C_a/r_2 = 0.002$, and using Eq. (47), we get $C_a = 0.004$ in.

## Acknowledgments

The authors are thankful to D. Hamrin, G. Rouse, G. Priddie, and M. Chinta at Capstone Turbine Corporation for providing information related to geometry and raw test data to compare and validate theoretical results.

## References

[1]Mugele, K., "Side-Channel Ring Compressor," U.S. Patent 3,973,865, 10 Aug. 1976.

[2]Wilson, W. A., Santalo, M. A., and Oelrich, J. A., "A Theory of the Fluid-dynamic Mechanism of Regenerative Pumps," *Transactions of the American Society of Mechanical Engineers*, Nov. 1955, pp. 1303–1316.

[3]Raheel, M., "A Theoretical, Experimental and CFD Analysis of Regenerative Flow Compressors and Regenerative Flow Pumps for Microturbine and Automotive Fuel Applications," Ph.D. Dissertation, Dept. of Mechanical Engineering, Michigan State Univ., East Lansing, MI, Dec. 2003.

[4]El Hag, A. I., "A Theoretical Analysis of the Flow in Regenerative Pumps," Ph.D. Dissertation, Univ. of Bath, Bath, England, U.K., 1979.

[5]Cates, P. S., "Peripheral-Compressor Performance on Gases With Molecular Weights of 4 to 400," American Society of Mechanical Engineers, ASME Transactions 64-WA/FE-25, Nov.–Dec. 1964.

[6]Raheel, M., Engeda, A., Hamrin, D., and Rouse, G., "The Performance Characteristics of Single-Stage and Multistage Regenerative Flow Compressors for Natural Gas Compression Application," *Journal of Mechanical Engineering Science*, Vol. 217, No. 11, 2003, pp. 1221–1240.

[7]Burton, D. W., "Review of Regenerative Compressor Theory," *Rotating Machinery for Gas-Cooled Reactor Application*, TID-7631, April 1962, pp. 228–242.

[8]Iversen, H. W., "Performance of the Periphery Pump," *Transactions of the American Society of Mechanical Engineers*, Vol. 77, Jan. 1955, pp. 19–28.

[9]Mason, S. C., "Influence of Internal Geometry upon Regenerative Pump Performance," B. S. Thesis, Dept. of Mechanical Engineering, Massachusetts Inst. of Technology, Cambridge, MA, May 1957.